Transmission through multiply-connected wire systems

D. Kowal
School of Physics and Astronomy, Raymond and Beverly Sackler Faculty of Exact Sciences, Tel-Aviv University, 69 978 Tel-Aviv, Israel
and Racah Institute of Physics, Hebrew University of Jerusalem, 91 904 Jerusalem, Israel

U. Sivan
School of Physics and Astronomy, Raymond and Beverly Sackler Faculty of Exact Sciences, Tel-Aviv University, 69 978 Tel-Aviv, Israel
and Thomas J. Watson IBM Research Center, P.O. Box 218, Yorktown Heights, New York 10598

O. Entin-Wohlman
School of Physics and Astronomy, Raymond and Beverly Sackler Faculty of Exact Sciences, Tel-Aviv University, 69 978 Tel-Aviv, Israel

Y. Imry
Department of Nuclear Physics, Weizmann Institute of Science, 76 100 Rehovot, Israel
(Received 20 July 1989; revised manuscript received 7 August 1990)

Employing a Landauer-type picture, the chemical potential at a certain site in a multiply-connected wire system is expressed in terms of the transmission amplitudes between this site and the external electron reservoirs. The result is applied to geometries involving rings containing magnetic flux, in order to derive nonlocal quantum interference effects in the conductance. As an example, h/e oscillations are obtained in the conductance of a wire with a "dangling ring" and in the conductance of a resistor in series with a ring. The general form of the scattering matrix of a three-terminal "fork" governing the transmission of a ring is found and exemplified by an explicit calculation within the tight-binding model. This example shows that, in general, the scattering matrix is not real (as assumed in previous studies), but that the qualitative results are not sensitive to the detailed form of the matrix.

I. INTRODUCTION

The purpose of this paper is to study the magnetoconductance of multiply-connected disordered structures made of one-dimensional (1D) wires. Such geometries involve junctions, wires, and loops[1,2] connecting several terminals. By the term "junction" we mean a part of the system from which several wires emerge. These junctions are usually described by scattering matrices,[3] and the matrix elements of those satisfy certain relations dictated by current conservation and other relevant symmetries.[4–7] The simplest example of a junction is a two-terminal one, described by a 2×2 scattering matrix. In the Landauer-type picture for the conductance[8,9] the sample itself is treated as a two-terminal junction, and its conductance is given in terms of the transmission coefficient T. A three-terminal junction is described by a 3×3 scattering matrix. In previous studies of transmission through rings[1,2] it was assumed that the scattering matrix of a fork with two identical arms can be taken to be real. Due to the current conservation condition, it then turned out that the scattering matrix was given by a single real parameter. However, the condition of current conservation imposed upon the scattering matrix of such a fork yields, quite generally, that the matrix is given by four real parameters. It is therefore of interest to construct an explicit example for the scattering matrix in order to check whether the previously made reality assumption is not too restrictive.

Using two- and three-terminal junctions as "building blocks," it is possible to construct and analyze more complicated geometries, in which quantum-mechanical effects in the conductance may occur. A simple example is a junction with three leads, only two of which are connected to external measurement probes [see Fig. 1(a)]. In such a system the "dangling" lead[1] affects the transmission coefficient, and hence the resistance. This comes about through interference between the part of the wave function which passes straight through the junction, and the part which is reflected back from the dangling lead. This is a nonlocal effect not expected in classical considerations.

As another example consider two barriers connected in a series [see Fig. 1(b)]. Using an expression for the local chemical potential, measured at a certain "site" in a system, it will be shown that each barrier can affect the measured resistance of the other. By the term site we mean a finite piece of the wire longer than the screening length and the electron wavelength, e.g., a tight-binding site or group of sites. One can define a local chemical potential only on such scales, where averaging over wave-function phases is possible. An expression for the local chemical

potential can be given in terms of the site wave function,[10] but its use involves the full wave-function calculation of the system. In Sec. II we show that in simple cases the chemical potential at a site can be expressed in terms of the transmission and reflection amplitudes between the site and the right and left external electron reservoirs. Using this expression we can study the magnetoconductance of the various parts of our system, provided that we know the transmission amplitudes of its constituents.

Other systems of interest are those involving rings.[1,2,11] Magnetic flux through a ring changes the interference between the parts of the wave function traversing the two branches of the ring, bringing about periodic oscillations in the transmission amplitude. This, in turn, can cause oscillatory nonlocal effects in other parts of the system. Two such systems are analyzed in Sec. III.

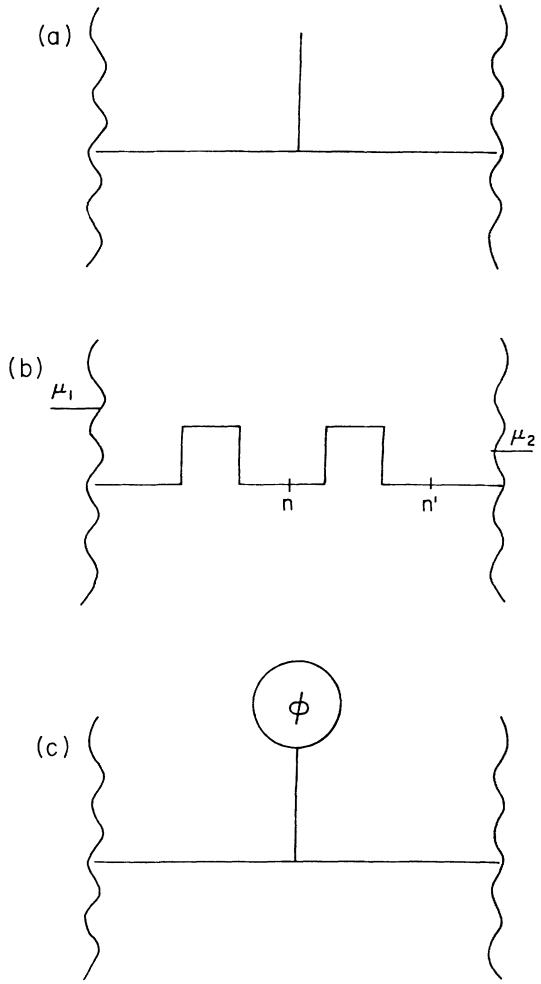

FIG. 1. (a) Schematic representation of a dangling wire connected to leads. Quantum-mechanical reflections of the electron wave functions from the end of the wire affect the resistance of the intersection. (b) Two barriers in a series in the Landauer picture. Interference effects cause each barrier to affect the resistance measured across the other. (c) Dangling ring. Flux through the ring changes the total transmission along the horizontal wire.

In Sec. II we investigate the scattering matrices of simple two- and three-terminal scatterers in the tight-binding (TB) model,[10,12] and discuss the number of parameters necessary to describe these matrices. The TB scattering matrix obtained for the three-terminal junction is in general complex. This shows that the assumption of a real scattering matrix made in previous ring transmission studies[1,2] is too restrictive, although it does not appear to affect qualitatively the calculated transmission through rings. In Sec. III we derive the transfer matrix of a ring containing magnetic flux, and the transfer matrix of a junction of a wire with a dangling ring [Fig. 1(c)]. The effect of these two systems on a barrier connected in a series to them (see insets to Figs. 4 and 5) is then calculated. These cases exemplify nonlocal quantum interference effects in the conductance. Such nonlocal effects have recently been obtained experimentally.[13,14] Section IV includes our conclusions. In the Appendix we discuss for completeness the scattering matrix[7] which describes a junction with inequivalent input and output channels.

II. THE CHEMICAL POTENTIAL INSIDE A CURRENT-CARRYING 1D CONDUCTOR

In the Landauer picture for the conductance of a disordered system [see Fig. 1(b)], the sample is connected by "ideal" wires to two electron reservoirs, of chemical potentials $\tilde{\mu}_L$ and $\tilde{\mu}_R$, respectively.[8,9] $\tilde{\mu}_L$ and $\tilde{\mu}_R$ are also the effective chemical potentials characterizing the channels flowing out of the reservoirs on the ideal wires. These reservoirs supply the external current flowing in the system. The chemical potential at a certain site, where a site is a piece of the system larger than the appropriate screening length and the electron wavelength, is defined as follows (at $T=0$ K). We weakly connect another reservoir to this site and adjust its chemical potential so that no current flows between the reservoir and the system. The chemical potential of the site under consideration is then defined as that of the measurement reservoir. In this way the local chemical potential can be defined for a system which is not in equilibrium. We emphasize that the above definition of the local chemical potential involves a "noninvasive" measurement by a probe which is so weakly coupled to the system that its influence on the system is negligible. This is different from ordinary "voltage probes" used in many experiments which do influence the system.[15] The recent technique of the scanning tunneling microscopy voltage measurement[16] demonstrates that such a procedure is feasible. In view of the recent emphasis in the literature[15] on voltage measurements with "invasive" probes that are strongly coupled to the system (as is the case in many current measurements) we stress that the concept of a local chemical potential is, however, well defined and useful. This concept is based on Refs. 8, 9, 17, and 18, where a local electrochemical potential is defined on scales much larger than the electron wavelength and the screening length after self-consistent screening has occurred. This can be measured by a weakly coupled probe, as first suggested in Ref. 18. The assumptions involved are that[10,19,20] the strength of the coupling to the weak probe

is proportional to the absolute value squared of the wave function at the measured site, or to the amplitude squared of the traveling "channel" waves in the case of ideal conductors. It then has to be assumed[20] that the strengths of the coupling to all channels at both directions are equal. This assumption is valid only after averaging over the length scales mentioned above, or possibly over a range of energies. This problem will be more fully discussed in Refs. 21 and 22. The possibility of such a measurement will be shown in Ref. 21 rigorously for the single-channel case and strong arguments for it will be given in the multichannel case.

For a weakly coupled probe it can be shown[10] that the chemical potential μ_n at site n [Fig. 1(b)] is given by

$$\mu_n=\frac{\tilde{\mu}_L\langle|\phi_n^L|^2\rangle+\tilde{\mu}_R\langle|\phi_n^R|^2\rangle}{\langle|\phi_n^L|^2\rangle+\langle|\phi_n^R|^2\rangle} . \tag{1}$$

Here $\langle|\phi_n^{L,R}|^2\rangle$ are the averages of the absolute value squared of the wave functions. The average is carried out over a wavelength, or a screening length (see below). The wave function ϕ_n^L is defined as follows. Consider the scattering state of the system defined by a wave emitted with unit amplitude from the left reservoir towards the right one. To the left of the system, in the ideal wire, the wave function has an amplitude of ϕ^L for the wave moving to the right, and $r\phi^L$ for the reflected wave moving to the left. To the right of the system, this scattering state is a wave of amplitude $t\phi^L$, moving to the right. We denote the amplitude of this scattering state at site n by ϕ_n^L. Similarly, the amplitude at site n of the scattering state emanating with unit amplitude from the right reservoir towards the left one is denoted ϕ_n^R. This scattering state has amplitudes ϕ^R and $r'\phi^R$ on the right-hand side of the system (for the waves moving to the left and to the right, respectively) and $t'\phi^R$ on the left-hand side (for the wave moving to the left). We emphasize that μ_n is a property of the site, *not* of the wave functions $\phi^{L,R}$. The values of the latter are used to determine μ_n.

This general form for the chemical potential has been previously[10,23] exploited to study the Hall-type voltage of a small disordered sample. However, its use involves the full quantum solution of the system. But for the simple geometries of the type portrayed in Fig. 1(b) and in the insets of Figs. 4 and 5, one is able to express the local chemical potential in terms of transmission and reflection amplitudes.

Let us denote the transfer matrix of a scatterer by τ, and the scattering matrix by σ. In general, σ and τ have the forms

$$\sigma=\begin{pmatrix} r & t' \\ t & r' \end{pmatrix},\quad \tau=\frac{1}{t'}\begin{pmatrix} tt'-rr' & r' \\ -r & 1 \end{pmatrix},\quad \det\tau=\frac{t}{t'} . \tag{2}$$

Current conservation implies that σ is unitary and that $|\det\tau|=1$ when the input and output channels are equivalent. But when, for example, the channels have different electron velocities, the elements of σ have to be modified by factors depending on these velocities, to make σ unitary (as well as to make $|\det\tau|=1$). These modifications, which amount to considering "current amplitudes" instead of wave functions, are discussed in the Appendix.

We now derive an expression for the local chemical potential in terms of the scattering parameters of the system. We take the wave functions entering the system of scatterers from the left and right in Fig. 1(b) to have unit amplitudes and take the wires connecting the system to the reservoirs to be equivalent. We denote the transfer matrix to the left of the site considered by τ_L, and that of the part to its right by τ_R. Clearly, the transmission matrix of the whole system, τ, is equal to $\tau_R\tau_L$, but note that the determinants $\det\tau_L$ and $\det\tau_R$ do not necessarily have unit magnitude when the central wire is different from the external leads. A specific example is considered in Sec. III. It shows that when the transfer integrals in the tight-binding (TB) model are J_1 on the two external leads and J_2 on the central wire, then $\det\tau_L=(\det\tau_R)^{-1}=(J_1\sin q_1/J_2\sin q_2)$, q_1 and q_2 being the electron wave numbers in the external and central wires, respectively.

The wave function ϕ_n^L at site n can be written as the linear combination $A_L e^{inq}+B_L e^{-inq}$, where q is the wave number of the scattering states and we take the lattice distance to be unity. The absolute value squared of the wave function contains cross terms which may not be completely eliminated by averaging over a wavelength,[24] causing oscillations in the measured chemical potential. In the following we will assume that such effects are relatively small and ignore the cross terms. This could be regarded as using a "phase-insensitive" probe.[24] The averaging procedure involved in the chemical-potential measurements[18] then implies that

$$\langle|\phi_n^L|^2\rangle=|A_L|^2+|B_L|^2 ,$$
$$\langle|\phi_n^R|^2\rangle=|A_R|^2+|B_R|^2 . \tag{3}$$

Having averaged over these quantities, no further averaging process is required. To find $\langle|\phi_n^L|^2\rangle$ and $\langle|\phi_n^R|^2\rangle$ in terms of the scattering parameters, we note that

$$\begin{pmatrix} A_R \\ B_R \end{pmatrix}=\tau_L\begin{pmatrix} 0 \\ t' \end{pmatrix} , \tag{4a}$$

$$\begin{pmatrix} t \\ 0 \end{pmatrix}=\tau_R\begin{pmatrix} A_L \\ B_L \end{pmatrix} . \tag{4b}$$

Using Eq. (2) we then find

$$|A_R|^2+|B_R|^2=\frac{|t'|^2}{|t_L'|^2}(1+|r_L'|^2) \tag{5}$$

and

$$|A_L|^2+|B_L|^2=\frac{|t|^2}{|t_R|^2}(1+|r_R|^2) . \tag{6}$$

Here we have used the total transmission amplitudes from the right (t') and from the left (t), obtained by multiplying two transfer matrices of the form (2),

$$t'=t_L'\frac{t_R'}{1-r_R r_L'},\quad t=t_R\frac{t_L}{1-r_L r_R'} . \tag{7}$$

The local electron density, obtained from Eqs. (5) and

(6), can be very low for certain wave numbers, but averaging over all the wave numbers will yield a density close to the average electron density of the material. This can be easily understood by considering the case of two high and narrow barriers separated by a distance L. We take all the wires in the system to be identical. If the barriers are taken to be high enough, the scattering amplitudes will depend on the wave number of an incident electron through the phase factors e^{iqL} and e^{2iqL} for $t_L t_R$ and $r_L r_R$, respectively. The density (6) will have a maximal value between the barriers at the resonances, i.e., whenever $|t|$ is maximal ($|1-r_R r_L'|$ is at a minimum). Altogether, this occurs $q_F(L/\pi)$ times for $E<E_F$, which is just the number of electrons expected to be in the wire between the barriers.

Inserting Eqs. (5) and (6) into Eq. (1) we obtain the chemical potential at site n [see (Fig. 1(b)] in terms of the scattering parameters of the various parts of the system

$$\mu_n=\frac{\tilde{\mu}_L|t|^2|t_L'|^2(1+|r_R|^2)+\tilde{\mu}_R|t'|^2t_R|^2(1+|r_L'|^2)}{|t|^2|t_L'|^2(1+|r_R|^2)+|t'|^2|t_R|^2(1+|r_L'|^2)} . \tag{8}$$

If the two leads to the system are equivalent then $|t|=|t'|$ and we are left with[18]

$$\mu_n=\frac{\tilde{\mu}_L|t_L'|^2(1+|r_R|^2)+\tilde{\mu}_R|t_R|^2(1+|r_L'|^2)}{|t_L'|^2(1+|r_R|^2)+|t_R|^2(1+|r_L'|^2)} . \tag{9}$$

We now exploit this expression to derive the conductance of parts of our structures. Consider two barriers in a series [see Fig. 1(b)]. For simplicity we assume that the central wire in Fig. 1(b) is identical to the external leads. The local chemical potential at site n' can be derived from Eq. (9) by considering the system as a whole to be the left scatterer, and the right scatterer to have unit transmission amplitude. The chemical-potential difference across the right barrier is then

$$\mu_n-\mu_{n'}=\frac{\tilde{\mu}_L-\tilde{\mu}_R}{2}\left(\frac{\frac{2}{T_R}-1}{\frac{1}{T_R}+\frac{1}{T_L}-1}-T\right) . \tag{10}$$

Here T, T_L, and T_R are the transmission coefficients of the entire system, the left and the right scatterers, respectively. A similar expression gives the potential drop across the left barrier. In reality, the potential drop across a barrier is brought about by a piling up of charges to its left and right, and by the electrostatic fields of these charges. These static charges do not participate in the conduction, and they disturb the constant potentials in the wires only within a screening length of the barriers. Further away charge neutrality is conserved because of the strong electrostatic forces, leading to self-consistent screening.[8,17]

The local chemical potential between the two scatterers may be lower than the local chemical potentials on the leads connecting the system to the external reservoirs, but will always be between $\tilde{\mu}_L$ and $\tilde{\mu}_R$. The current through the system is equal to the electron charge multiplied by the number of electrons participating in the conduction per unit length and by the electron velocity. In a one-dimensional system the density of states per unit energy is $1/\pi\hbar v$, where v is the electron velocity. Thus, the total current, including spin degeneracy, is[8,9]

$$j=(\tilde{\mu}_L-\tilde{\mu}_R)\frac{e}{\pi\hbar}T . \tag{11}$$

Dividing the current by the voltage drop across a part of the system gives the conductance of that part. The conductance of the right barrier is thus

$$G_2=\frac{e^2}{\pi\hbar}T\frac{\tilde{\mu}_L-\tilde{\mu}_R}{\mu_n-\mu_{n'}}=\frac{2e^2}{\pi\hbar}\frac{-1+\frac{1}{T_R}+\frac{1}{T_L}}{1-\frac{1}{T}-\frac{1}{T_L}-\frac{1}{T_R}+\frac{2}{T_RT}} . \tag{12}$$

The results obtained in this way are different from the classical conductances. The conductance of an element in a system can be larger than the conductance of that element alone. The conductance of a part of a system can be negative, although the conductance of the system as a whole, given by the usual Landauer formula,[8,9] is always positive. Since the whole system is coherent and electron thermalization and energy dissipation occur in the reservoirs alone,[9,20] only the total conductance must be positive.[21] In general, the conductances of the various elements of a system are affected by the scattering properties of all the other elements. The relative effects will be greatest when the scattering coefficients of the various elements are of similar magnitude. Oscillations (e.g., of the Aharonov-Bohm type) in the scattering amplitudes of one of the elements will cause oscillations, to a varying degree, in the conductances of the other elements.

An example of the use of Eq. (12) is given in Sec. III. We emphasize that these nonlocal effects are intrinsic to the system and have nothing to do with the measurement probes.

III. THE TRANSFER AND SCATTERING MATRICES IN PARTICULAR CASES

A. General treatment of the scattering and transfer matrices

In this section we calculate the 2×2 and 3×3 scattering matrices in the TB model for specific configurations. We start by looking at a discontinuity along a TB chain [see Fig. 2(a)]. Denoting the wave function at site n by ϕ_n, the TB equations are

$$(\varepsilon_n-E)\phi_n=\sum_{n'}J_{n,n'}\phi_{n+n'} , \tag{13}$$

where the sum runs over the nearest neighbors of n, ε_n is the site energy, J is the transfer integral between nearest neighbors, and E is the single electron energy.

Consider first the solution of Eq. (13) for a system composed of two semi-infinite, ordered chains of site energies ε_1 and ε_2 and transfer integrals J_1 and J_2, respectively, connected at site M of site energy ε_M [see Fig. 2(a)].

Choosing J_1 and J_2 to be real, Eq. (13) yields

$$\begin{bmatrix}\phi_{n+1}\\ \phi_n\end{bmatrix}=\begin{bmatrix}\alpha_i & -1\\ 1 & 0\end{bmatrix}\begin{bmatrix}\phi_n\\ \phi_{n-1}\end{bmatrix},$$
$$\alpha_i=\frac{\varepsilon_i-E}{J_i},\quad i=1,2\ , \tag{14}$$

for $n\neq M$, and

$$\begin{bmatrix}\phi_{M+1}\\ \\ \phi_M\end{bmatrix}=\begin{bmatrix}\dfrac{\varepsilon_M-E}{J_2} & -\dfrac{J_1}{J_2}\\ 1 & 0\end{bmatrix}\begin{bmatrix}\phi_M\\ \\ \phi_{M-1}\end{bmatrix}, \tag{15}$$

for $n=M$. We seek the traveling wave solutions of these equations. To this end we write

$$\phi_n=\begin{cases}A_1e^{iq_1n}+B_1e^{-iq_1n}, & n\leq M \quad (16a)\\ A_2e^{iq_2n}+B_2e^{-iq_2n}, & n\geq M\ . \quad (16b)\end{cases}$$

Equation (14) then implies $\alpha_1=2\cos q_1$ and $\alpha_2=2\cos q_2$, which relates q_i to the energy E of the electron, while Eq. (15) yields the transfer matrix at site M:

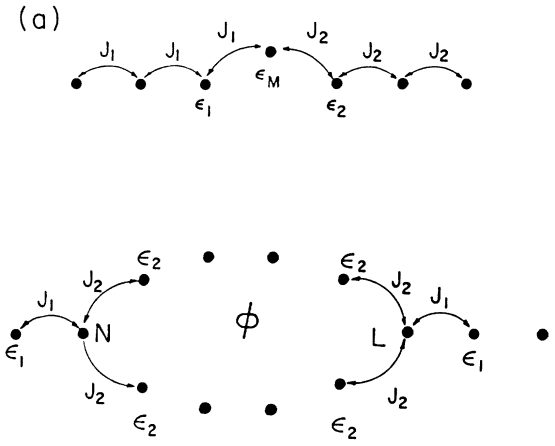

FIG. 2. (a) Simple barrier in the tight-binding model. The wires to the left and right have site energies ε_1 and ε_2, and transfer integrals J_1 and J_2, respectively. The site energy at the barrier site M is ε_M. (b) Ring in the tight-binding model. The ring junctions are situated at sites N and L. The leads have site energies ε_1 and transfer integrals J_1. The wires in the ring have parameters ε_2 and J_2.

$$\begin{bmatrix}A_2\\ B_2\end{bmatrix}=\tau_M\begin{bmatrix}A_1\\ B_1\end{bmatrix},$$
$$\tau_M=\frac{1}{2iJ_2\sin q_2}\begin{bmatrix}(\varepsilon_M-E-J_1e^{-iq_1}-J_2e^{-iq_2})e^{i(q_1-q_2)M} & (\varepsilon_M-E-J_1e^{iq_1}-J_2e^{-iq_2})e^{-i(q_1+q_2)M}\\ (E-\varepsilon_M+J_1e^{-iq_1}+J_2e^{iq_2})e^{i(q_1+q_2)M} & (E-\varepsilon_M+J_1e^{iq_1}+J_2e^{iq_2})e^{i(q_2-q_1)M}\end{bmatrix}. \tag{17}$$

As detailed in the Appendix, multiplying τ_M by velocity-dependent factors will yield a transfer matrix which relates the "current amplitudes" scattered by the system. Let v_1 and v_2 be the electron velocities in the wires to the left and right of the scatterer, $v_1=(2/\hbar)J_1\sin q_1$, $v_2=(2/\hbar)J_2\sin q_2$, respectively. The matrix $\mathcal{T}_M=(v_2/v_1)^{1/2}\tau_M$ can be shown to have a unit determinant. For $M=0$, $\mathcal{T}_0$ is given by four real parameters, which is the minimal number of parameters needed to describe a general transfer matrix.

We now construct a unitary scattering matrix in the TB model[12] for a three-terminal splitter, for the case in which the scattering into and from two of the branches, numbered 2 and 3, is the same (see left-hand side of Fig. 2(b). We start by reviewing the general properties of 3×3 unitary scattering matrices with two equivalent branches,[2]

$$\mathcal{S}=\begin{bmatrix}c & \sqrt{\kappa} & \sqrt{\kappa}\\ \sqrt{\kappa} & a & b\\ \sqrt{\kappa} & b & a\end{bmatrix}, \tag{18}$$

where all four parameters are, in general, complex. The parameters are related[2] by equations arising from the unitarity of $\mathcal{S}$,

$$|c|^2+2|\kappa|=1\ ,$$
$$|\kappa|+|a|^2+|b|^2=1\ , \tag{19}$$
$$c\sqrt{\kappa^*}+(a^*+b^*)\sqrt{\kappa}=|\kappa|+ab^*+a^*b=0\ .$$

The solution of these equations yields that, in general, $\mathcal{S}$

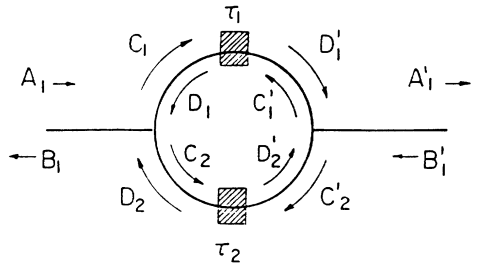

FIG. 3. Schematic model of a ring with scattering in the branches. Ideal leads are joined by splitters to a ring with two scatterers.

is given by four independent real parameters,

$$c=-e^{-i\gamma+i\beta}\sqrt{1-2\rho},\quad \sqrt{\kappa}=e^{i\beta/2}\sqrt{\rho}\ ,$$
$$a=\frac{1}{2}(e^{i\gamma}\sqrt{1-2\rho}+e^{i\alpha}),\quad b=\frac{1}{2}(e^{i\gamma}\sqrt{1-2\rho}-e^{i\alpha})\ , \tag{20}$$
$$0<\rho<\tfrac{1}{2},\quad 0<\alpha,\beta,\gamma<2\pi\ .$$

One of these parameters can be chosen as an overall phase factor of the matrix.

We now derive the scattering matrix of a junction connecting three TB ordered chains, of which two are identical and are described by site energies ε_2 and transfer integrals J_2. The third chain is different and has site energies ε_1 and transfer integrals J_1 [see Fig. 2(b)]. This scattering matrix and the scattering matrix for a mirror image junction, will be used to obtain the transmission and reflectance of a TB ring threaded by a magnetic flux (Fig. 2(b).

Referring to Fig. 3, the traveling wave solutions are

$$\phi_n=A_1e^{iq_1n}+B_1e^{-iq_1n},\quad n\le N\ , \tag{21a}$$
$$\phi_n^{(1)}=C_1e^{iq_2n}+D_1e^{-iq_2n},\quad n\ge N\ , \tag{21b}$$
$$\phi_n^{(2)}=C_2e^{iq_2n}+D_2e^{-iq_2n},\quad n\ge N\ . \tag{21c}$$

Inserting these into the TB equation (13), we find

$$E-\varepsilon_1=-2J_1\cos q_1;\ E-\varepsilon_2=-2J_2\cos q_2\ , \tag{22}$$

which relates the electron wave number to the wire parameters and electron energy, and

$$\begin{bmatrix}B_1\\C_1\\C_2\end{bmatrix}=\sigma_N\begin{bmatrix}A_1\\D_1\\D_2\end{bmatrix}\ ,$$

where

$$\sigma_N=\begin{bmatrix}\left[\frac{2iJ_1\sin q_1}{D}-1\right]e^{2iq_1N} & \frac{2iJ_2\sin q_2}{D}e^{i(q_1-q_2)N} & \frac{2iJ_2\sin q_2}{D}e^{i(q_1-q_2)N}\\ \frac{2iJ_1\sin q_1}{D}e^{i(q_1-q_2)N} & \left[\frac{2iJ_2\sin q_2}{D}-1\right]e^{-2iq_2N} & \frac{2iJ_2\sin q_2}{D}e^{-2iq_2N}\\ \frac{2iJ_1\sin q_1}{D}e^{i(q_1-q_2)N} & \frac{2iJ_2\sin q_2}{D}e^{-2iq_2N} & \left[\frac{2iJ_2\sin q_2}{D}-1\right]e^{-2iq_2N}\end{bmatrix}\ ,$$
$$D=E-\varepsilon_N+J_1e^{iq_1}+2J_2e^{iq_2}\ . \tag{23}$$

In the Appendix it is shown that a unitary scattering matrix $\mathcal{S}_N$ may be obtained from (23), using Eq. (A8), thereby giving a specific example of the general form (18). For $N=0$, $\mathcal{S}_0$ can be described by three real parameters, one less than is necessary for the general 3×3 scattering matrix obtained above [see Eq. (20)]. This means that there are three-terminal junctions which cannot be described by the simple TB scatterer we have analyzed.

B. A tight-binding ring

We calculate the transmission of the ring in Fig. 2(b) using current amplitudes. To take the magnetic field into account, we have to replace the transfer integrals on the upper arm by $J_{n,n+1}\to J_{n,n+1}e^{i\theta}$, and on the lower arm by $J_{n,n+1}\to J_{n,n+1}e^{-i\theta}$. Here the phase θ is chosen such that the total phase change in going once around the ring is equal to the total flux through the ring divided by $\Phi_0=ch/e$. We also have to multiply the traveling wave solutions of the upper and lower branches [Eq. (20)] by $e^{in\theta}$ and $e^{-in\theta}$, respectively. This leads to a scattering matrix of the general form

$$\mathcal{S}_N=\begin{bmatrix}c_N & \sqrt{\kappa_N}e^{-iN\theta} & \sqrt{\kappa_N}e^{iN\theta}\\ \sqrt{\kappa_N}e^{iN\theta} & a_N & b_Ne^{2iN\theta}\\ \sqrt{\kappa_N}e^{-iN\theta} & b_Ne^{-2iN\theta} & a_N\end{bmatrix}\ . \tag{24}$$

The dependence of the parameters c_N, κ_N, a_N, and b_N on N is given by

$$a_N=e^{-2iq_2N}a,\quad b_N=e^{-2iq_2N}b\ ,$$
$$c_N=e^{2iq_1N}c,\quad \sqrt{\kappa_N}=\sqrt{\kappa}e^{i(q_1-q_2)N}\ . \tag{25}$$

For the mirror image fork on the right-hand side of the ring, situated at site L, the scattering matrix can be obtained from Eqs. (24) and (25) by making the following exchanges [see Fig. 2(b)]: $D_1'\leftrightarrow D_2$, $C_1'\leftrightarrow C_2$, $A_1'\leftrightarrow B_1$, $D_2'\leftrightarrow D_1$, $C_2'\leftrightarrow C_1$, $B_1'\leftrightarrow A_1$. The general form obtained for $\mathcal{S}_L$ is the same as (24), with $-L$ exchanging N.

The transmission amplitude of a ring is found by solving the linear equations given by the scattering matrices (24) of the ring junctions and the scattering matrices describing the arms of the ring. In other words, there is a dependence of A_1' and B_1' on A_1 and B_1. In this calculation, the amplitudes A, B, C, and D, as well as the matrices, refer to current amplitudes (see the Appendix).

The scattering matrix (24) can be used to find the transfer amplitudes between the two arms of the ring, with an additional term due to the external left branch

$$\begin{bmatrix}D_2\\C_2\end{bmatrix}=e^{-2iN\theta}s_N\begin{bmatrix}C_1\\D_1\end{bmatrix}+e^{-iN\theta}A_1\mathbf{v}_N\ , \tag{26}$$

where

$$s_N=\frac{1}{b_N}\begin{bmatrix}1 & -a_N\\ a_N & b_N^2-a_N^2\end{bmatrix},\quad \mathbf{v}_N=\frac{\sqrt{\kappa_N}}{b_N}\begin{bmatrix}1\\ b_N-a_N\end{bmatrix}. \tag{27}$$

In addition, Eq. (24) gives

$$B_1=\left[c_N-\frac{\kappa_N}{b_N}\right]A_1+e^{-iN\theta}\mathbf{u}_N\begin{bmatrix}C_1\\ D_1\end{bmatrix},$$
$$\mathbf{u}_N=\frac{\sqrt{\kappa_N}}{b_N}(1,\ b_N-a_N)\,. \tag{28}$$

The left-hand side of the ring is described by analogous equations

$$\begin{bmatrix}D_2'\\ C_2'\end{bmatrix}=e^{-2iL\theta}s_{-L}\begin{bmatrix}C_1'\\ D_1'\end{bmatrix}+e^{-iL\theta}B_1'\mathbf{v}_{-L}\,; \tag{29}$$

s_{-L} and $\mathbf{v}_{-L}$ are defined in the same manner as (27), but with $-L$ replacing N there, and similarly,

$$A_1'=\left[c_{-L}-\frac{\kappa_{-L}}{b_{-L}}\right]B_1'+e^{-iL\theta}\mathbf{u}_{-L}\begin{bmatrix}C_1'\\ D_1'\end{bmatrix}, \tag{30}$$

where u_{-L} is given by $\mathbf{u}_N$ [Eq. (28)] with $-L$ replacing N.

Assuming scattering along the arms of the ring, the waves along the upper and lower branches are related by transfer matrices τ_1 and τ_2, respectively,

$$\begin{bmatrix}D_1'\\ C_1'\end{bmatrix}=\tau_1\begin{bmatrix}C_1\\ D_1\end{bmatrix},\quad \begin{bmatrix}D_2'\\ C_2'\end{bmatrix}=\tau_2\begin{bmatrix}C_2\\ D_2\end{bmatrix}. \tag{31}$$

These relations give

$$B_1=A_1\left[c_N-\frac{\kappa_N}{b_N}-e^{i\phi}\mathbf{u}_N P\mathbf{v}_N\right]+B_1'e^{i\phi/2}\mathbf{u}_N P\begin{bmatrix}0 & 1\\ 1 & 0\end{bmatrix}\tau_2^{-1}\mathbf{v}_{-L}\,, \tag{32}$$

where

$$P=\left[e^{i\phi}s_N-\begin{bmatrix}0 & 1\\ 1 & 0\end{bmatrix}\tau_2^{-1}s_{-L}\begin{bmatrix}0 & 1\\ 1 & 0\end{bmatrix}\tau_1\right]^{-1} \tag{33}$$

and $\phi=2(L-N)\theta$. This relates three of the current amplitudes entering and leaving the ring. Similarly, Eqs. (26)–(30) give

$$A_1'=B_1'\left[c_{-L}-\frac{\kappa_{-L}}{b_{-L}}+\mathbf{u}_{-L}\begin{bmatrix}0 & 1\\ 1 & 0\end{bmatrix}\tau_1 P\begin{bmatrix}0 & 1\\ 1 & 0\end{bmatrix}\tau_2^{-1}\mathbf{v}_{-L}\right]-A_1\mathbf{u}_{-L}\begin{bmatrix}0 & 1\\ 1 & 0\end{bmatrix}\tau_1 P\mathbf{v}_N e^{i\phi/2}\,. \tag{34}$$

From Eqs. (33) and (34) one obtains the scattering amplitudes of the ring. Consider for simplicity the case in which the scattering matrices of the two junctions of the ring are described by the same TB parameters, apart from the phases related to their locations. Then the parameters a, b, c, and κ [Eq. (25)] describing the left junction are the same as those used to describe the right junction. We calculate the reflection and transmission amplitudes of the ring for the case of no scattering along the branches, i.e., τ_1 and τ_2 being unit matrices. From the symmetry of such a ring it is clear that the reflection and transmission amplitudes of the whole ring will be the same, for waves coming from the left- and from the right-hand sides. Under these conditions the reflection and transmission amplitudes of the ring are

$$r=c_N-\frac{\kappa_N}{b_N}-e^{i\phi}\mathbf{u}_N P\mathbf{v}_N$$
$$=e^{2iq_1N}\left[c-\frac{2\kappa}{d}\left[b\cos\phi+a-e^{i\psi}(b^2-a^2)(b-a)\right]\right],$$
$$t=2\kappa e^{i(q_1-q_2)(N-L)}\frac{\cos(\phi/2)}{d}[(b-a)^2-e^{-i\psi}]\,, \tag{35}$$

where $d=2b^2\cos\phi-e^{-i\psi}-(b^2-a^2)^2e^{i\psi}+2a^2$ and $\psi=2q_2(L-N)$. Since the wires on both sides of the ring were chosen to be identical, the reflection and transmission coefficients obtained for the current amplitudes are the coefficients for the wave functions as well. Equations (35) are generalizations of the expressions obtained by Buttiker *et al.*[2] for a simpler ring, and has the same general properties. We make use of these expressions in the following subsections. Expressions for the transmission and reflection amplitudes of rings with scattering along the arms appear in Ref. 25.

C. A dangling ring

As an example of a nonlocal effect, consider the case of a dangling ring with no scattering inside it [see Fig. 1(c)]. Here one is interested in the conduction along the horizontal wire. The ring at the end of the vertical wire brings about a phase shift between the waves entering and those leaving this wire. This relationship, together with the 3×3 scattering matrix of the junction to the ring, leads to an equivalent 2×2 scattering matrix for the waves on the main wire. In order to calculate the phase shift at the main junction we need to know how the ring affects the phase of the reflected wave at the entrance to the ring. This is found by eliminating the wire leaving the ring of Fig. 3 from the right. For a scattering-free ring we obtain

$$B_1=A_1e^{2iq_1N}\left[c-2\kappa\frac{\cos\phi-e^{i\psi}(b-a)}{2b\cos\phi-e^{-i\psi}-e^{i\psi}(b^2-a^2)}\right]$$
$$\equiv A_1Z\,. \tag{36}$$

Using the relationships (19), the absolute value of Z can be shown to be 1, as expected. Its phase can be interpreted as that of the reflection amplitude at the junction of the wire and the ring in Fig. 1(c). We now calculate the effect of the dangling ring on the transfer matrix of the junction on the main wire. For simplicity, all the wires are taken to be identical. Therefore the scattering and transfer matrices for wave functions and current amplitudes are identical. For an intersection at N', which is symmetrical with respect to the two branches lying on the main wire, the relationships between incoming and outgoing waves are

$$
\begin{aligned}
B_1 &= \frac{Z\sqrt{\kappa_{N'}}}{1-c_{N'}Z}(D_3+D_4)\ , \\
C_3 &= D_3\left[a_{N'}+\frac{Z\kappa_{N'}}{1-c_{N'}Z}\right] \\
&\quad +D_4\left[b_{N'}+\frac{Z\kappa_{N'}}{1-c_{N'}Z}\right]=rD_3+t'D_4\ , \qquad (37)\\
C_4 &= D_3\left[b_{N'}+\frac{Z\kappa_{N'}}{1-c_{N'}Z}\right] \\
&\quad +D_4\left[a_{N'}+\frac{Z\kappa_{N'}}{1-c_{N'}Z}\right]=tD_3+r'D_4\ .
\end{aligned}
$$

It is seen that $t=t'$ and $r=r'$. The wave functions along the main wire are related by a transfer matrix τ, whose matrix elements are

$$
\begin{aligned}
\tau_{12}=\tau_{21}^{*} &= -\frac{a_{N'}+Z(\kappa_{N'}-a_{N'}c_{N'})}{b_{N'}+Z(\kappa_{N'}-b_{N'}c_{N'})}\ , \\
\tau_{22}=\tau_{11}^{*} &= \frac{1-c_{N'}Z}{b_{N'}+Z(\kappa_{N'}-b_{N'}c_{N'})}\ .
\end{aligned}
\qquad (38)
$$

These results effectively replace the dangling ring by a flux sensitive barrier.

D. A barrier in a series with a ring

We now consider a further example for a nonlocal effect, namely, a barrier in a series with a ring (see inset of Fig. 4). Using the expressions derived in Sec. II for the conductances of parts of complex systems, we can find the conductance of the barrier itself. Examples of the results thus obtained are shown in Fig. 4. The oscillations of the scattering amplitudes of the ring, as a function of the magnetic flux through it, cause oscillations in the conductance of the barrier.

E. A barrier in series with a dangling ring

In a completely analogous way we can find the conductance of the barrier when the ring is replaced by a dangling ring (see inset of Fig. 5), by inserting values from Eq. (38). The oscillations in the barrier's conductance will not necessarily be greatest when there is no scattering between the ring and the junction on the main wire. As stated in Sec. II, such effects depend on the relative

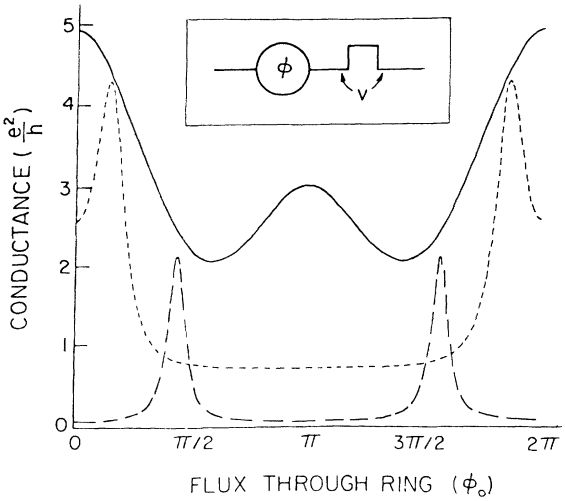

FIG. 4. A barrier in a series with a ring (see inset) in the tight-binding model. The conductance plotted is that of the barrier alone, defined as the ratio of the current to the voltage across the barrier. The ring is situated at site 0 and has branches of length 2. The barrier is situated at site 5. $J_1=1$ for all lines. Solid line: $E=1$; $J_2=1$; $E_{\text{barrier}}=1$. Dashed line: $E=1$; $J_2=2$; $E_{\text{barrier}}=5$. Dotted line: $E=0.5$; $J_2=2$; $E_{\text{barrier}}=1$.

magnitude of the effective scattering coefficients of the barrier on the main wire and the junction with the vertical wire. Sample results are shown in Fig. 5. These results demonstrate the variety of behaviors possible for this nonlocal effect. Oscillations in similar systems have been observed experimentally by Umbach *et al.*,[13] and by

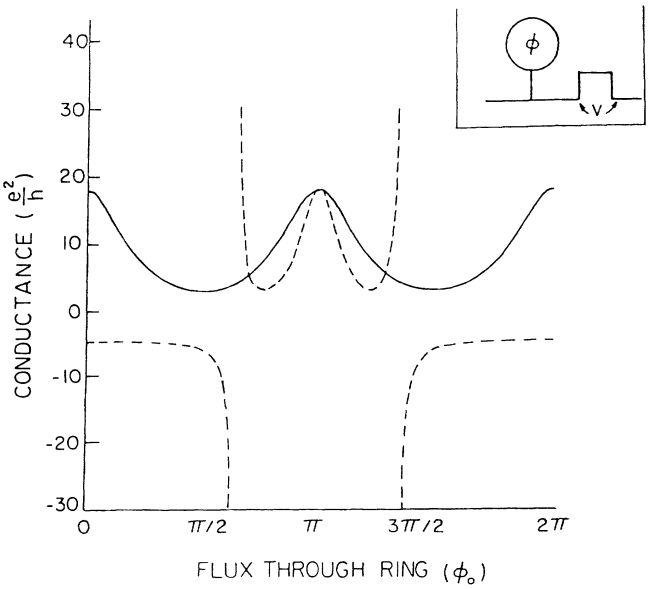

FIG. 5. A barrier in a series with a dangling ring in the tight-binding model (see inset). The conductance is of the barrier alone. The junction on the main wire is at site 0, the ring is three sites away with branches of length 2 and the barrier is at site 3. $E=1$, $J_1=1$, and $E_{\text{barrier}}=1$ for all lines. Solid line: $J_2=1$. Dashed line: $J_2=2$, chosen to represent a case where the inverse conductance vanishes and changes signs at a point.

Webb *et al.*[14] In the experiments of Umbach *et al.* the resistance of a piece of wire oscillated when in a series with a dangling ring. Webb *et al.* found the resistances of two rings in a series to be affected by each other.

IV. DISCUSSION

Two main points were demonstrated in this paper. The first is that one may construct scattering matrices of a multiply-connected wire system in a systematic way, making use of the TB Hamiltonian. The second is that chemical-potential differences can be expressed in terms of scattering matrix elements. These were used to derive two nonlocal effects in composite conductors, namely, the resistance of a dangling ring, and the effect of a ring on a resistor series connected to it. These nonlocal effects are intrinsic to the system itself and are not related to measurement probes. Chemical-potential differences between various sites in a sample expressed in terms of scattering matrix elements could turn out to be useful for studying Hall conductances. In Sec. II we considered a simple example, in which we exploited 2×2 scattering matrices. Similar methods can be used for studying more complicated geometries, using, for example, 3×3 scattering matrices. We hope to pursue this point in the future.

ACKNOWLEDGMENTS

This research was partially supported by the Fund for Basic Research administered by the Israel Academy of Sciences and Humanities and by the Minerva Foundation, Munich, the Federal Republic of Germany. We thank R. Landauer and Y. Gefen for helpful discussions.

APPENDIX: CURRENT CONSERVATION CONSIDERATIONS

When the scattering in the sample is taken to be elastic, the current in any energy interval is conserved. The current entering the scatterer from both sides at a given energy is

$$j_{\rm in}=e[\langle|\phi^L(E)|^2\rangle v_1(E)+\langle|\phi^R(E)|^2\rangle v_2(E)]\ , \tag{A1}$$

where v_1 and v_2 are the Fermi velocities in the wires on the left and right of the system, respectively, and ϕ_L and ϕ_R are as defined in Sec. II. Equation (A1) can be written as the electron charge, e, times the squared absolute value of the vector

$$\mathbf{w}_{\rm in}=\begin{bmatrix}\sqrt{v_1(E)} & 0\\ 0 & \sqrt{v_2(E)}\end{bmatrix}\begin{bmatrix}\phi^L(E)\\ \phi^R(E)\end{bmatrix}\ . \tag{A2}$$

The current leaving the scatterer at the same energy is

$$j_{\rm out}=e[v_1(E)\langle|\phi^L(E)r+\phi^R(E)t'|^2\rangle + v_2(E)\langle|\phi^L(E)t+\phi^R(E)r'|^2\rangle]\ . \tag{A3}$$

This can be written as e times the squared absolute value of

$$\mathbf{w}_{\rm out}=\begin{bmatrix}\sqrt{v_1(E)} & 0\\ 0 & \sqrt{v_2(E)}\end{bmatrix}\sigma\begin{bmatrix}\phi^L(E)\\ \phi^R(E)\end{bmatrix}=\begin{bmatrix}\sqrt{v_1(E)} & 0\\ 0 & \sqrt{v_2(E)}\end{bmatrix}\sigma\begin{bmatrix}\sqrt{v_1(E)^{-1}} & 0\\ 0 & \sqrt{v_2(E)^{-1}}\end{bmatrix}\times\begin{bmatrix}\sqrt{v_1(E)} & 0\\ 0 & \sqrt{v_2(E)}\end{bmatrix}\begin{bmatrix}\phi^L(E)\\ \phi^R(E)\end{bmatrix}\ . \tag{A4}$$

Defining a matrix $\mathcal{S}$ as

$$\mathcal{S}=V\sigma V^{-1},\quad V=\begin{bmatrix}\sqrt{v_1(E)} & 0\\ 0 & \sqrt{v_2(E)}\end{bmatrix}\ , \tag{A5}$$

Eq. (A4) becomes

$$\mathbf{w}_{\rm out}=\mathcal{S}\mathbf{w}_{\rm in}\ . \tag{A6}$$

The requirement of current conservation implies that $\mathcal{S}$ is unitary, and can therefore be more convenient to use than the original matrix σ relating the wave-function amplitudes. Since the squared magnitude of the vectors $\mathbf{w}_{\rm in}$ and $\mathbf{w}_{\rm out}$ are proportional to the current, we term them current amplitudes. The unitarity of $\mathcal{S}$ leads to the relationship $|r|=|r'|$.

The transfer matrix associated with $\mathcal{S}$ is given by

$$\mathcal{T}=\tau\begin{bmatrix}v_2\\ v_1\end{bmatrix}^{1/2}\ . \tag{A7}$$

A similar matrix can be derived for a three-terminal junction. If σ_3 is the S matrix for the wave functions, then

$$\mathcal{S}_3=\begin{bmatrix}v_1^{1/2} & 0 & 0\\ 0 & v_2^{1/2} & 0\\ 0 & 0 & v_3^{1/2}\end{bmatrix}\sigma_3\begin{bmatrix}v_1^{-1/2} & 0 & 0\\ 0 & v_2^{-1/2} & 0\\ 0 & 0 & v_3^{-1/2}\end{bmatrix} \tag{A8}$$

is a unitary matrix. In practice, the wave-function scattering and transfer matrices of the various scatterers and splitters of a system are found from the Schrödinger equation. The unitary matrices obtained from them can

then be used to calculate the conductance of the system as a whole. The $\sqrt{v}$ factors between elements inside the system cancel out. Therefore, calculations made with the unitary matrices are equivalent to those made with the original matrices (relating wave-function amplitudes) except that the final result can be used to calculate the currents directly. The wave-function scattering and transfer matrices of the entire system can be obtained using Eqs. (A5) and (A7) in reverse. Note that when v_1 is equal to v_2, $\mathcal{S}$ is equal to σ. The unitarity of $\mathcal{S}$ implies that $|\det \mathcal{T}|=1$. This can be interpreted as a change in the normalization (see Fisher and Lee[7]).

[1]Y. Gefen, Y. Imry, and M. Ya. Azbel, Phys. Rev. Lett. **52**, 129 (1984).
[2]M. Büttiker, Y. Imry, and M. Ya. Azbel, Phys. Rev. A **30**, 1982 (1984).
[3]B. Shapiro, Phys. Rev. Lett. **50**, 747 (1983).
[4]P. W. Anderson, D. J. Thouless, E. Abrahams, and D. S. Fisher, Phys. Rev. B **22**, 3519 (1980).
[5]D. C. Langreth and E. Abrahams, Phys. Rev. B **24**, 2978 (1981).
[6]P. A. Lee and D. S. Fisher, Phys. Rev. Lett. **47**, 882 (1981).
[7]D. S. Fisher and P. A. Lee, Phys. Rev. B **23**, 6851 (1981).
[8]R. Landauer, IBM J. Res. Develop. **1**, 223 (1957).
[9]R. Landauer, Philos. Mag. **21**, 863 (1970).
[10]O. Entin-Wohlman, C. Hartzstein, and Y. Imry, Phys. Rev. B **34**, 921 (1986).
[11]R. A. Webb, S. Washburn, C. P. Umbach, and R. B. Laibowitz, Phys. Rev. Lett. **54**, 2696 (1985); V. Chandrasekhar, M. J. Rooks, S. Wind, and D. E. Prober, *ibid.* **55**, 1610 (1985).
[12]B. Doucot and R. Rammal, J. Phys. (Paris) **48**, 941 (1987).
[13]C. P. Umbach, P. Santhanam, C. van Haesendonck, and R. A. Webb, Appl. Phys. Lett. **50**, 1289 (1987).
[14]R. A. Webb, S. Washburn, H. J. Haucke, A. D. Benoit, C. P. Umbach, and F. P. Milliken, in Proceedings of the Fifth International Winter School, *Austria, 1988,* edited by H. Heinrich, G. Bauer, and F. Kuchar (Springer, Heidelberg, 1988), p. 98.
[15]M. Buttiker, Phys. Rev. B **33**, 3020 (1986).
[16]J. R. Kirtley, S. Washburn, and M. J. Brady, Phys. Rev. Lett. **60**, 1546 (1988), contains references to previous work.
[17]M. Buttiker, R. Landauer, Y. Imry, and S. Pinhas, Phys. Rev. B **31**, 6207 (1985).
[18]H. L. Engquist and P. W. Anderson, Phys. Rev. B **24**, 1151 (1981).
[19]J. Tersoff and D. R. Hamann, Phys. Rev. Lett. **50**, 1998 (1983); Phys. Rev. B **31**, 805 (1985).
[20]U. Sivan and Y. Imry, Phys. Rev. B **33**, 551 (1986). U. Sivan, Ph.D. thesis, Tel-Aviv University, 1988.
[21]U. Sivan and Y. Imry (unpublished).
[22]R. Landauer, Z. Phys. B **68**, 217 (1987); J. Phys. C **1**, 8099 (1989); in *Analogies in Optics and Microelectronics,* edited by W. van Haeringen and D. Lenstra (Kluwer Academic, The Netherlands, 1990), p. 243.
[23]U. Sivan, Y. Imry, and C. Hartzstein, Phys. Rev. B **39**, 1242 (1988).
[24]M. Büttiker, Phys. Rev. B **40**, 3409 (1990).
[25]D. Kowal, M.Sc. thesis, Tel-Aviv University, 1988.